

Noisy signal propagation and amplification in phenotypic transition cascade of colonic cellsXue-fen Hou , Bin-qian Zhou , Yi-fan Zhou , Charles Omotomide Apata , Long Jiang , and Qi-ming Pei ^{*}
School of Physics and Optoelectronic Engineering, Yangtze University, Jingzhou 434023, China (Received 21 August 2020; revised 27 October 2020; accepted 10 November 2020; published 9 December 2020)

Like genes and proteins, cells can use biochemical networks to sense and process information. The differentiation of the cell state in colonic crypts forms a typical unidirectional phenotypic transitional cascade, in which stem cells differentiate into the transit-amplifying cells (TACs), and TACs continue to differentiate into fully differentiated cells. In order to quantitatively describe the relationship between the noise of each compartment and the amplification of signals, the gain factor is introduced, and the gain-fluctuation relation is obtained by using the linear noise approximation of the master equation. Through the simulation of these theoretical formulas, the characters of noise propagation and amplification are studied. It is found that the transmitted noise is an important part of the total noise in each downstream cell. Therefore, a small number of downstream cells can only cause its small inherent noise, but the total noise may be very large due to the transmitted noise. The influence of the transmitted noise may be the indirect cause of colon cancer. In addition, the total noise of the downstream cells always has a minimum value. As long as a reasonable value of the gain factor is selected, the number of cells in colonic crypts will be controlled within the normal range. This may be a good method to intervene the uncontrollable growth of tumor cells and effectively control the deterioration of colon cancer.

DOI: [10.1103/PhysRevE.102.062411](https://doi.org/10.1103/PhysRevE.102.062411)**I. INTRODUCTION**

Signal transduction plays an important role in cell-to-cell communication, thereby affecting cell survival, proliferation, differentiation, and death behavior. For example, through protein-protein activation, the cytoskeleton and nucleus can transmit signals from the cell surface to various intracellular destinations, thereby causing phenotypic changes [1]. Ras-MAPK (mitogen-activated protein kinase) signal transduction pathway can activate gene expression and change cell growth characteristics [2,3]. The famous Michaelis-Menten equation behaves like a molecular switch [4–6], and it acts as a key signal amplifier in the regulation of cell proliferation or apoptosis [7]. All in all, the signaling transduction is closely related to tissue growth and differentiation, protein synthesis and secretion, the composition of intracellular and extracellular fluid, metabolic processes, and so on [8].

The signal transduction pathway also controls and maintains normal physiological balance. In a healthy organism, the process of cell growth and differentiation is strictly controlled. But under pathological conditions, it loses control and causes further damage signals, or the growth of malfunctioning cells. The proliferation of damaged or dysfunctional cells is often a key factor in the development of diseases such as cancer, infectious diseases, inflammation, arteriosclerosis, arthritis, and neurodegenerative diseases.

Noise permeates all levels of biological systems [9–12]. Due to the intrinsic noise originating from the random occurrence of biochemical reactions or the extrinsic noise generating from the microenvironment, the biochemical process in a single cell may fluctuate [13,14]. Therefore, the

signal transduction system is inherently noisy [6,15,16]. The stochastic nature of the input signal during the signal transduction process in living cells had already been revealed using single-molecule detection technique [5,15–22].

In order to explore how the signal system operates under stochastic fluctuations, a great deal of work has been done in the past 20 y. As early as 2000, the noise in signal transduction was discussed, and the results showed that large amplification would cause strong random fluctuations in the output signal [23,24]. Research on the ultrasensitive signal cascade operating near saturation showed that even if the noisy cascade length is large, the output signal fluctuation will be bounded in magnitude, and the noise can be attenuated [22]. Paulsson's series of work showed that cells can exploit signal noise to reduce the random variation in regulatory processes [25], signal noise can attenuate the concentration noise in a regulated component [26], and the noise generated in a reaction can propagate in signal transduction networks [27]. In 2005, Shibata and Fujimoto proposed the gain-fluctuation relation in order to theoretically deal with the relationship between noise and the signal amplification in the process of intracellular signal transduction [6]. In 2008, the gain-fluctuation relation was applied to some typical signal systems, and it was found that the noise in the signal transduction system restricted the chemotaxis of cells and caused their behavior variability [15]. Using the standard Ω -extension technique to study the stochastic fluctuations in the protein synthesis cascade, the results show that for any given protein species, the contribution of upstream protein fluctuations to its noise should be additive [28]. The interaction network between genes and proteins shows that positive feedback as a central element can buffer the propagation of noise while maintaining sensitivity to long-term changes in the input signal [29]. In 2012, an abstract model of the Myc/E2F/MiR-17-92 network

^{*}qmpei@yangtzeu.edu.cn

was analyzed, suggesting that the negative (positive) feedback mechanism in coupled feedback loop can dynamically buffer noise impact, not just suppress or amplify the noise [30]. Based on the combination of global sensitivity analysis and stochastic simulations, a systematic method to characterize noise propagation in the cascade was developed [7]. Later, another intuitive but fully quantitative method was proposed to analyze how noise affects the phenotype of cells. It was found that noise can simultaneously enhance the sensitivity in one behavioral region and reduce the sensitivity in another [13]. In 2014, using information theory to evaluate the channel capacity of the complex promoter architecture and comparing it with the baseline provided by the two-state model, the results show that, except in certain cases, adding internal states to the promoter generally reduces the channel capacity [31]. One year later, the theoretical analysis of switchlike promoters revealed that the ability of the circuit to attenuate noise is a trade-off between the strength of suppression and that of the promoter [32]. In 2017, analysis based on single-cell microscopy showed that noise can interact synergistically with oscillatory dynamics, thereby enhancing the sensitivity of signal processing [33].

Quantifying biochemical processes at the cellular level is becoming the central task of modern molecular biology [13]. Like genes and proteins, cells can also use biochemical networks to sense and process information [29].

Therefore, interesting questions are pointed out: How does the noise of cells in biochemical networks relates to the amplification of signals? What is the main source of total noise in cells? To address these issues, we choose a unidirectional phenotypic transition cascade in a colonic crypt [34–36] as an example of a stochastic computation system. As in the gene expression cascade, the upstream cells are used as input signals, the downstream cells are used as output signals, and a gain factor [6,14–17,27,29,37] is introduced to obtain the gain-fluctuation equation, which can quantitatively describe the propagation of the noise in the phenotypic transition cascade. Moreover, the noise amplification ratio [7,30,31] between the output signal and the input signal is obtained.

Gillespie's algorithm [38] is a classic approach for stochastic simulation of chemical systems [32]. It is usually used to test whether the theoretical results are correct, because this algorithm can give statistically accurate simulations. In our work, all data are compared with those of the Gillespie algorithm.

The paper is arranged as follows. We start by constructing a unidirectional phenotypic transition cascade in a colonic crypt in Sec. II. In Sec. III, the gain-fluctuation relation for theoretically analyzing how noise relates to the signal amplification in the phenotypic transition cascade of colonic crypt is derived by using the linear noise approximation of the master equation [39,40]. By virtue of these theoretical formulas, the effect of the gain on noise propagation and amplification is studied in Sec. IV. We end with conclusions and discussions in Sec. V.

II. UNIDIRECTIONAL PHENOTYPIC TRANSITION CASCADE IN A COLONIC CRYPT

Consider a model of differentiations of cell states in a colonic crypt. There are three compartments containing stem

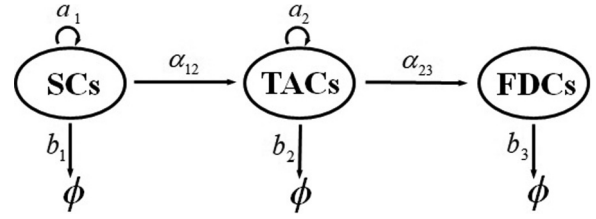


FIG. 1. A schematic diagram of differentiations from SCs to TACs and then to FDCs in a colonic crypt.

cells (SCs), transit-amplifying cells (TACs), and fully differentiated cells (FDCs) [35–37], as shown in Fig. 1. SCs undergo renew, death, and differentiate into TACs with the probabilities per unit time a_1 , b_1 , and α_{12} , respectively. And, TACs undergo renew, death, and differentiate with the probabilities per unit time a_2 , b_2 , and α_{23} , respectively. FDCs come from the differentiation of TACs and are removed with the probability per unit time b_3 . In order to maintain the cell population under the equilibrium in the crypt, the transition rates among the different phenotypes are taken as $\alpha_{12} = \alpha_0 + k_1 N_1 / (1 + m_1 N_1)$ with an inherent transition rate α_0 , and $\alpha_{23} = \beta_0 + k_2 N_2 / (1 + m_2 N_2)$ with an inherent transition rate β_0 , in which k_i and m_i ($i = 1, 2$) are non-negative constants, where k_i represents the speed of response of the feedback and m_i represents feedback saturation. With the increasing of the population SCs (or TACs), its differentiation rate is increased until to a maximum value. So, this feedback mechanism is named the saturating feedback. Here we take the dimensionless parameters $a_2 = 0.5$, $b_1 = b_2 = 0.1$, $b_3 = 0.323$, $\alpha_0 = 0.1$, $\beta_0 = 0.2$, $k_1 = m_1 = 0.1$, $k_2 = m_2 = 0.01$ [34–36,41].

In the deterministic description, the time evolution of the cell population can be written

$$\begin{aligned} \frac{dN_1}{dt} &= a_1 N_1 - b_1 N_1 - \alpha_{12} N_1 \\ \frac{dN_2}{dt} &= a_2 N_2 - b_2 N_2 + \alpha_{12} N_1 - \alpha_{23} N_2 \\ \frac{dN_3}{dt} &= -b_3 N_3 + \alpha_{23} N_2, \end{aligned} \quad (1)$$

where N_1 , N_2 , N_3 are the numbers of SCs, TACs, and FDCs, respectively. Taking $dN_i/dt = 0$ ($i = 1, 2, 3$), the steady states N_i^s are obtained as follows:

$$\begin{aligned} N_1^s &= \frac{\alpha}{k_1 - m_1 \alpha} \\ N_2^s &= \frac{\beta + D m_2 + \sqrt{(\beta - D m_2)^2 + 4 D k_2}}{2(k_2 - m_2 \beta)} \\ N_3^s &= \frac{\alpha_{23}}{b_3} N_2^s, \end{aligned} \quad (2)$$

with $\alpha = a_1 - b_1 - \alpha_0$, $\beta = a_2 - b_2 - \beta_0$, $D = \alpha_{12} N_1^s$. Here α and β denote the inherent net (per-capita) growth rates of SCs and TACs, respectively. D is the differentiation rate of stem cells at the steady state. In order to ensure that the number of each cell population at steady state is a valid value, α and β should satisfy the following conditions:

$$0 < \alpha < \frac{k_1}{m_1}, \quad 0 < \beta < \frac{k_2}{m_2}. \quad (3)$$

III. GAIN-FLUCTUATION RELATION

A. Fokker-Planck equation

The joint probability distribution $P(N_1, N_2, N_3, t)$ of population kinetics Eq. (1) obeys the following master equation [39,40]:

$$\begin{aligned} \frac{\partial P}{\partial t} = & \sum_{i=1}^3 \left[(E_i^{-1} - 1) a_i N_i + (E_i^1 - 1) b_i N_i \right. \\ & \left. + \sum_{j \neq i} (E_j^1 E_i^{-1} - 1) \alpha_{ji} N_j + \sum_{j \neq i} (E_i^1 E_j^{-1}) \alpha_{ij} N_i \right] P, \end{aligned} \quad (4)$$

where E_i and E_j are the step operators acting on N_i and N_j , respectively. For a function $f(N_i, N_j)$ with two integer arguments, the step operator $E_i^{\pm m}$ (or $E_j^{\pm m}$) increases N_i (or N_j) by an integer $\pm m$, i.e., $E_i^{\pm m} f(N_i, N_j) = f(N_i \pm m, N_j)$, $E_j^{\pm m} f(N_i, N_j) = f(N_i, N_j \pm m)$.

The master equation cannot be solved accurately, so it is necessary to adopt a systematic approximation method. By using van Kampen's Ω -expansion method, the subpopulation is approximated by setting $N_i(t) = \Omega x_i(t) + \Omega^{1/2} \xi_i(t)$ for large system size Ω , and the joint probability distribution is written by $P(N_1, N_2, N_3, t) = \Omega^{-3/2} \Pi(\xi_1, \xi_2, \xi_3, t)$. Collecting the terms of Ω^0 in the expansion of Eq. (4) forms a linear Fokker-Planck equation,

$$\frac{\partial \Pi}{\partial t} = - \sum_{i,k} A_{ik} \frac{\partial}{\partial \xi_i} (\xi_k \Pi) + \frac{1}{2} \sum_{i,k} B_{ik} \frac{\partial^2 \Pi}{\partial \xi_i \partial \xi_k}, \quad (5)$$

where \mathbf{A} is the drift matrix and \mathbf{B} is the diffusion matrix. \mathbf{A} and \mathbf{B} depend on the stoichiometry of the transitions and the macroscopic rates. The matrix elements A_{ik} are defined by

$$A_{ik} = \frac{\partial}{\partial x_k} \left(a_i x_i - b_i x_i - \sum_{j \neq i} \alpha_{ij} x_i + \sum_{j \neq i} \alpha_{ji} x_j \right), \quad (6)$$

the matrix elements B_{ik} are defined by

$$\begin{aligned} B_{ii} &= 2 \left(a_i x_i + \sum_{j \neq i} \alpha_{ji} x_j \right), \\ B_{ik} &= -(\alpha_{ik} x_i + \alpha_{ki} x_k) \quad (k \neq i). \end{aligned} \quad (7)$$

B. Normalized fluctuation-dissipation formula

For stationary variances, the linear noise approximation is summarized by

$$\mathbf{AC} + (\mathbf{AC})^T + \Omega \mathbf{B} = 0, \quad (8)$$

where matrix \mathbf{C} contains both the variance C_{ii} which characterizes the fluctuation in population of the i th phenotype and the covariance C_{ik} which represents the degree of correlation between the noise in the i th subpopulation and that in the k th subpopulation. Equation (8) is named the fluctuation dissipation relationship.

To quantify the noise propagation in phenotypic transition cascades around the steady state, Eq. (8) is normalized as

$$\mathbf{MV} + (\mathbf{MV})^T + \mathbf{D} = 0, \quad (9)$$

with

$$V_{ik} = V_{ki} = \frac{C_{ik}}{\langle N_i \rangle \langle N_k \rangle}, \quad M_{ik} = A_{ik} \frac{\langle N_k \rangle}{\langle N_i \rangle}, \quad D_{ik} = \frac{\Omega B_{ik}}{\langle N_i \rangle \langle N_k \rangle}. \quad (10)$$

Angle brackets indicate average values. In the mean-field theory, the stationary population number can be replaced by its mean value, namely $N_i^s = \langle N_i \rangle$. Equation (9) is named the normalized fluctuation-dissipation formula.

By using Eq. (7) and Eq. (10), and taking into account $N_i(t) = \Omega x_i(t) + \Omega^{1/2} \xi_i(t)$, we have

$$\begin{aligned} D_{ii} &= \frac{2[a_i \langle N_i \rangle + \sum_{j \neq i} \alpha_{ji} \langle N_j \rangle]}{\langle N_i \rangle^2}, \\ D_{ik} &= - \left(\frac{\alpha_{ik}}{\langle N_k \rangle} + \frac{\alpha_{ki}}{\langle N_i \rangle} \right) \quad (k \neq i). \end{aligned} \quad (11)$$

C. The reaction flux elasticity

To measure how the balance between production and elimination of N_i is affected by N_k , the reaction flux elasticity [27,35–37] is defined by

$$H_{ki} = \left\langle \frac{\partial \ln(J_i^- / J_i^+)}{\partial \ln N_k} \right\rangle, \quad (12)$$

where $J_i^+ = a_i + \sum_{j \neq i} \alpha_{ji} N_j$ is the pure production rate of phenotype i and $J_i^- = b_i + \sum_{j \neq i} \alpha_{ij} N_i$ is the pure elimination rate of phenotype i . Equation (12) also can be rewritten as

$$H_{ki} = - \left\langle \frac{N_k}{J_i^+} \frac{\partial}{\partial N_k} (J_i^+ - J_i^-) \right\rangle. \quad (13)$$

Here, $J_i^+ - J_i^-$ is the net production rate of phenotype i .

Taking into account Eq. (1), we have $H_{13} = H_{21} = H_{31} = H_{32} = 0$, $H_{33} = 1$, and

$$\begin{aligned} H_{11} &= \frac{\alpha}{a_1} \left(1 - \frac{m_1}{k_1} \alpha \right), \\ H_{22} &= \frac{1}{b_2 + \alpha_{23}} \left[\frac{\alpha_{12} \langle N_1 \rangle}{\langle N_2 \rangle} + \frac{k_2 \langle N_2 \rangle}{(1 + m_2 \langle N_2 \rangle)^2} \right] \\ H_{12} &= - \frac{\langle N_1 \rangle}{\alpha_2 \langle N_2 \rangle + \alpha_{12} \langle N_1 \rangle} \left[\alpha_{12} + \frac{k_1 \langle N_1 \rangle}{(1 + m_1 \langle N_1 \rangle)^2} \right], \\ H_{23} &= - \frac{1}{\alpha_{23}} \left[\alpha_{23} + \frac{k_2 \langle N_2 \rangle}{(1 + m_2 \langle N_2 \rangle)^2} \right]. \end{aligned} \quad (14)$$

It can be seen that $H_{11}, H_{22} > 0$ and $H_{12}, H_{23} < 0$, because all parameters and mean values $\langle N_i \rangle$ are positive. Based on Eq. (13) and Eq. (14), it is shown that SCs or TACs can negatively regulate their own net production rates, while upstream cells can positively regulate the net production rates of their downstream cells. The former is because as their number increases, more and more SCs or TACs will differentiate, while the latter is because TACs (or FDCs) mainly come from the differentiation of SCs (or TACs).

D. The gain factor

In the signal transduction system, the noise amplification can be quantified by gain g , which is defined as the ratio of the relative change of the output signal to that of the input signal [6,14–17,27,29,37]. In the phenotypic transition cascade, we take the upstream cells as input signals and the downstream cells as output signals. So, the input and output signals are affected by the reaction process, which is different from the signal transduction system. Therefore, when the populations change very little, we redefine the gain factor based on the reaction flux as

$$g_{ik} = \left| \left\langle \frac{\Delta N_k / N_k}{\Delta N_i / N_i} \right\rangle \right| = \left| \left\langle \frac{\partial \ln N_k}{\partial \ln N_i} \right\rangle \right| = \left| \left\langle \frac{\partial \ln(J_k^- / J_k^+)}{\partial \ln N_i} \right\rangle \left\langle \frac{\partial \ln N_k}{\partial \ln(J_k^- / J_k^+)} \right\rangle \right| = \left| \frac{H_{ik}}{H_{kk}} \right|. \quad (15)$$

The sign of the absolute value ensures that the gain coefficient is positive, because it is known from Eq. (14) that the value of H_{12} or H_{23} may be negative. In our work, there are two gain factors as following:

$$g_{12} = \left| \frac{H_{12}}{H_{22}} \right| \equiv g_1, \quad g_{23} = \left| \frac{H_{23}}{H_{33}} \right| \equiv g_2. \quad (16)$$

They are called the first-order signal factor and the second-order signal factor, respectively.

E. Gain-fluctuation relation

Under the steady state, $\langle J_i^+ \rangle = \langle J_i^- \rangle = \langle J_i \rangle$, so that the average lifetime is determined by the subpopulation divided by the total rate of elimination,

$$\tau_i = \left\langle \frac{N_i}{J_i^-} \right\rangle = \left\langle \frac{N_i}{J_i^+} \right\rangle = \left\langle \frac{N_i}{J_i} \right\rangle. \quad (17)$$

For the three compartments SCs, TACs, and FDCs in a colonic crypt, their average lifetimes are, respectively,

$$\tau_1 = 1/a_1, \quad \tau_2 = 1/(b_2 + \alpha_{23}), \quad \tau_3 = 1/b_3. \quad (18)$$

Thus, the drift matrix \mathbf{A} and its normalized form \mathbf{M} at the steady state are rewritten, respectively, as

$$A_{ik} = \frac{\langle N_i \rangle}{\langle N_k \rangle} \Theta_i g_{ki}, \quad M_{ik} = A_{ik} \frac{\langle N_k \rangle}{\langle N_i \rangle} = g_{ki} \Theta_i, \quad (19)$$

where $\Theta_i = \langle \frac{\partial}{\partial N_i} (J_i^+ - J_i^-) \rangle$, which is the net production probability per unit time at the steady state, represents the change rate of net production rate with its own number, and reflects the influence of the i th phenotypic state on its own growth.

Substituting Eq. (11) and Eq. (19) into Eq. (9), we get

$$\sum_{j=1}^3 V_{ji} g_{ji} = -\frac{1}{\langle N_i \rangle \tau_i \Theta_i}, \quad (20)$$

$$\sum_{j=1}^3 (V_{jk} \Theta_i g_{ji} + V_{ij} \Theta_k g_{jk}) = \left[\frac{\alpha_{ik}}{\langle N_k \rangle} + \frac{\alpha_{ki}}{\langle N_i \rangle} \right] \quad (k \neq i). \quad (21)$$

Expanding Eq. (20) and Eq. (21) with $V_{ij} = V_{ji}$ ($i, j = 1, 2, 3$), $g_{12} \equiv g_1$, and $g_{23} \equiv g_2$, we can obtain the correlation between fluctuations in the i th phenotype and in the j th phenotype, that is normalized covariance V_{ij} ($i = 1, 2, 3; i \neq j$), as following:

$$V_{12} = V_{21} = -V_{11} g_1 \frac{\Theta_2}{\Theta_1 + \Theta_2} + \frac{\alpha_{12} / \langle N_2 \rangle}{\Theta_1 + \Theta_2}, \quad (22)$$

$$V_{13} = V_{31} = -V_{12} g_2 \frac{\Theta_3}{\Theta_1 + \Theta_3}, \quad (23)$$

$$V_{23} = V_{32} = -V_{13} g_1 \frac{\Theta_2}{\Theta_2 + \Theta_3} - V_{22} g_2 \frac{\Theta_3}{\Theta_2 + \Theta_3} + \frac{\alpha_{23} / \langle N_3 \rangle}{\Theta_2 + \Theta_3}. \quad (24)$$

Then, we can obtain normalized variations V_{ii} ($i = 1, 2, 3$), as following:

$$V_{11} = -\frac{1}{\langle N_1 \rangle \tau_1 \Theta_1}, \quad (25)$$

$$V_{22} = \underbrace{-\frac{1}{\langle N_2 \rangle \tau_2 \Theta_2}}_{\text{pure intrinsic noise}} + \underbrace{\left(-\frac{\alpha_{12} / \langle N_2 \rangle}{\Theta_1 + \Theta_2} g_1 \right)}_{\text{conversion noise between SCs and TACs}} + \underbrace{V_{11} \frac{\Theta_2}{\Theta_1 + \Theta_2} g_1^2}_{\text{transmitted noise from SCs}}, \quad (26)$$

$$V_{33} = \underbrace{-\frac{1}{\langle N_3 \rangle \Theta_3 \tau_3}}_{\text{pure intrinsic noise}} + \underbrace{V_{11} \frac{\Theta_2}{\Theta_1 + \Theta_2} \frac{\Theta_2}{\Theta_2 + \Theta_3} \frac{\Theta_3}{\Theta_1 + \Theta_3} g_1^2 g_2^2}_{\text{transmitted noise from SCs}} + \underbrace{V_{22} \frac{\Theta_3}{\Theta_2 + \Theta_3} g_2^2}_{\text{transmitted noise from TACs}} + \underbrace{\left(-\frac{\Theta_2}{\Theta_2 + \Theta_3} \frac{\Theta_3}{\Theta_1 + \Theta_3} \frac{\alpha_{12} / \langle N_2 \rangle}{\Theta_1 + \Theta_2} g_1 g_2^2 \right)}_{\text{conversion noise between SCs and TACs}} + \underbrace{\left(-\frac{\alpha_{23} / \langle N_3 \rangle}{\Theta_2 + \Theta_3} g_2 \right)}_{\text{conversion noise between TACs and FDCs}}. \quad (27)$$

V_{ii} represents the total noise in the i th phenotypic state. Equations (25)–(27) are gain-fluctuation relationship,

which indicates that the noise propagation along the signal cascade can be characterized by the gain factor

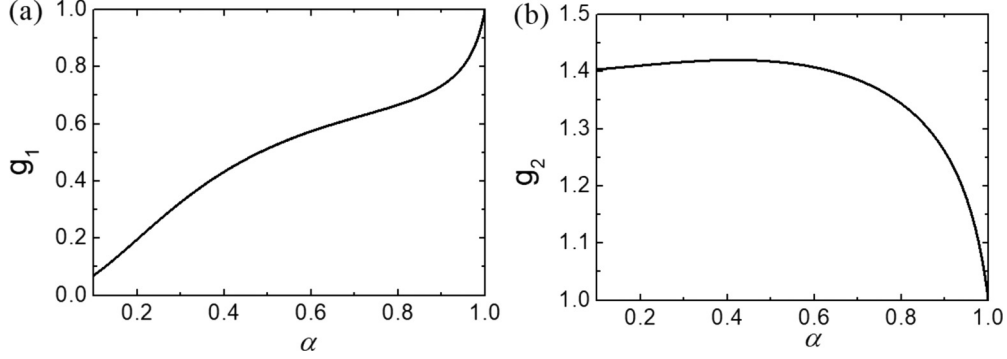


FIG. 2. Gain factors g_k ($k = 1, 2$) as a function of α . The other parameter values are given in the text. All the parameters are measured in hours^{-1} .

g_k ($k = 1, 2$), the characteristic time of the signal response $\Gamma_{il} = \Theta_i / (\Theta_i + \Theta_l)$, ($i = 2, 3; l = 1, 2, 3$, and $l \neq i$). It is also shown that the noise in the upstream cells can propagate to the downstream cells. And, the contribution of the fluctuation in the upstream cell to that in the downstream cell is additive. That is to say, the noise of the downstream cell can be expressed as a linear function of the noise of the upstream cell. The total noises in the i th phenotypic state include the intrinsic noise of the i th phenotypic state, the transmitted noise from the upstream phenotypes, and the interconversion noise.

E. Noise amplification rate

In the phenotypic transition cascade, we take upstream cells as input signals and downstream cells as output signals. When the upstream cell (i.e., the i th phenotype) fluctuates with the standard deviation σ_{ii} , and the downstream cell (i.e., the j th phenotype) fluctuates with the standard deviation σ_{jj} , the ratio of relative noise intensity gives the noise amplification rate [6,29,30] as follows:

$$A_{ij} = \frac{\sigma_{jj} / \langle N_j \rangle}{\sigma_{ii} / \langle N_i \rangle}. \quad (28)$$

In the fluctuation-dissipation formula [Eq. (8)], C_{ii} means the variance of fluctuations in the i th phenotype. Therefore,

$$C_{ii} = \sigma_{ii}^2. \quad (29)$$

Substituting Eq. (29) into Eq. (28) and considering Eq. (10), the noise amplification rate is redefined as

$$A_{ij} = \sqrt{\frac{V_{jj}}{V_{ii}}}. \quad (30)$$

Because the phenotypic transition cascade in colonic crypts is unidirectional, there are three noise amplification rates in our work as following:

$$\begin{aligned} A_{12} &= \sqrt{\frac{V_{22}}{V_{11}}} \equiv A_1, & A_{23} &= \sqrt{\frac{V_{33}}{V_{22}}} \equiv A_2, \\ A_{13} &= \sqrt{\frac{V_{33}}{V_{11}}} \equiv A_3. \end{aligned} \quad (31)$$

IV. SIMULATIONS AND RESULTS

A. The character of gain factors

The parameter α represents the inherent net (per-capita) growth rate of SCs. From Eq. (2), we can see that α affects the numbers of three cell populations. It is one of the key parameters in the phenotypic transition cascade of colonic crypts, so the parameter α is selected as the control variable.

The gain factors g_k ($k = 1, 2$) as a function of α are given in Fig. 2. It is shown from Fig. 2(a) that g_1 increases with the increase of α . In the whole parameter range, $0 < g_1 \leq 1$, which means the relative change of the output signal is smaller than that of the input signal. Therefore, the noise is attenuated from SCs to TACs. Figure 2(b) shows that g_2 decreases rapidly as α increases. In the whole parameter range, $g_2 \geq 1$, which means the relative change of the output signal is greater than that of the input signal. Therefore, the noise is amplified from TACs to FDCs.

B. Effects of gain factors on covariance

It can be seen from Eq. (22) that V_{12} seems to have a linear relationship with g_1 . However, g_1 is closely related to the numbers of SCs N_1 and TACs N_2 . Therefore, it is difficult to directly judge the relationship between them based on these expressions. It can be seen from Eq. (23) and Eq. (24) that V_{23} and V_{13} are the same.

The three-dimensional graphs of α , g_k ($k = 1, 2$) and normalized covariance V_{ij} ($i = 1, 2, 3; i \neq j$) are shown in Figs. 3(a) and 3(c). The corresponding projection of each graph on the $g_k - V_{ij}$ plane is shown in Figs. 3(b) and 3(d). It can be shown that $V_{12}, V_{13}, V_{23} > 0$. So, there is a positive correlation between the fluctuations in any two of three phenotypic states. The responses of V_{12}, V_{23} , and V_{13} to changes in g_1 or g_2 are similar. Each curve in Fig. 3(b) is approximately a parabola with upward opening, and its lowest point is approximately at $g_1 = 0.6$. It means that when the first-order signal factor is 0.6, the correlation between any two fluctuations in three phenotypic states is the weakest. Each curve in Fig. 3(c) is an asymmetric deformed parabola with an upward opening, and its lowest point is approximately at $g_1 = 1.4$. It is suggested that when the second-order signal factor is 1.4, the correlation between any two fluctuations in three phenotypic states is the weakest.

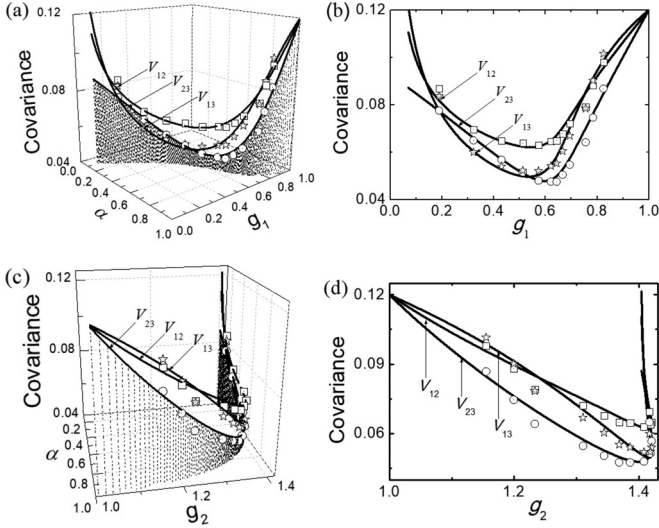


FIG. 3. Effects of gain factors g_k ($k = 1, 2$) on normalized covariances V_{ij} ($i = 1, 2, 3; i \neq j$). (a), (c) Three-dimensional figures of α , g_k , and V_{ij} ; (b), (d) corresponding projection figures on the g_k - V_{ij} plane. Lines are theoretical predictions according to Eqs. (22)–(24). Hollow markers are from simulations using the Gillespie method [39]. The other parameter values are given in the text. All the parameters are measured in hours⁻¹.

C. Effects of gain factor on fluctuations

The three-dimensional graphs of α , g_k ($k = 1, 2$) and normalized variance V_{ii} ($i = 2, 3$) are shown in Figs. 4(a) and 4(c). The corresponding projection of each graph on the g_k - V_{ii} plane is shown in Figs. 4(b) and 4(d). It can be seen from Fig. 4(b) that as g_1 increases, the normalized variance of TACs V_{22} first

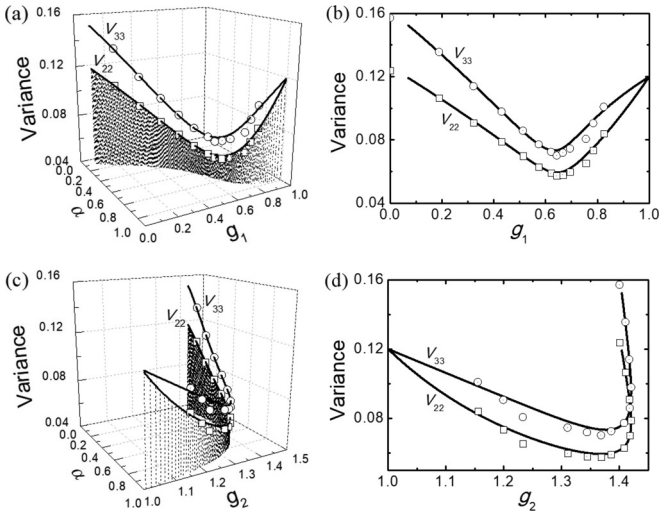


FIG. 4. Effects of gain factors g_k ($k = 1, 2$) on normalized variances V_{ii} ($i = 2, 3$). (a), (c): Three-dimensional figure of α , g_k , and V_{ii} ; (b), (d): Corresponding projection figures on the g_k - V_{ii} plane. Lines are theoretical predictions according to Eqs. (26) and (27). Hollow markers are from simulations using the Gillespie method [39]. The other parameter values are given in the text. All the parameters are measured in hours⁻¹.

decreases, reaches the minimum nearly at $g_1 = 0.65$, and then increased to 0.12.

The shape of V_{33} is similar. V_{22} and V_{33} reach their minimums almost synchronously at $g_1 = 0.65$. In particular, for each g_1 , the value of V_{33} is greater than that of V_{22} , which means that the relative fluctuation of FDCs (i.e., the noise in FDCs) is stronger than that in TACs.

With the increase of g_2 , the normalized variance of TACs V_{22} or FDCs V_{33} first decreases, reaches the minimum nearly at $g_1 = 1.40$, and then rapidly increases to 0.12 or 0.16, as shown in Fig. 4(d). Comparing the two curves, we can find for the most of g_2 , the value of V_{33} is greater than that of V_{22} . So, in most cases, the noise in FDCs is stronger than that in TACs.

Thus, with the increase of g_1 or g_2 , the changes of V_{22} and V_{33} are synchronous. Therefore, we can adjust g_1 or g_2 to obtain the smallest noises in TACs and in FDCs, thereby regulating their population under control. Relatively speaking, g_1 is better than g_2 in regulating the noise of TACs or FDCs.

D. Effects of gain factor on noise propagation

Using Eqs. (25)–(27), the effect of gain factors g_k ($k = 1, 2$) on noise propagation in three cell states are discussed by Eq. (25) shows that the total noise in SCs is only pure intrinsic noise, because there is no random fluctuation environment provided by other compartments. Equation (26) or Eq. (27) shows that the total noise of TACs or FDCs can be decomposed into intrinsic noise, transmitted noise, and conversion noise. The pure intrinsic noise $(N_i \tau_i \Theta_i)^{-1}$ of TACs ($i = 2$) or FDCs ($i = 3$) depends on its low numbers N_i , the average lifetime τ_i , and the net production probability per unit time at the steady state Θ_i . The transmitted noise of TACs comes from the intrinsic noise of SCs, and the conversion noise of TACs is caused by the differentiation from SCs to TACs. The transmitted noise of FDCs includes two parts: One comes from the intrinsic noise of SCs, and the other comes from the total noise of TACs. The conversion noise of FDCs is also composed of two parts: One comes from the differentiation from TACs to FDCs, and the other comes from the differentiation from SCs to TACs, respectively.

The corresponding simulation result is shown in Fig. 5. As g_1 increases, the intrinsic noise of TACs decreases, the transmitted noise from SCs increases, and the conversion noise between SCs and TACs is almost zero, as shown in Fig. 5(a). With g_2 increases, the intrinsic noise of TACs increases, the transmitted noise from SCs decreases, and the conversion noise between SCs and TACs is almost zero, as shown in Fig. 5(c). Therefore, whether it is g_1 or g_2 , the total noise of TACs depends on both intrinsic noise and transmitted noise.

As g_1 increases, the intrinsic noise of FDCs, the conversion noise between SCs and TACs, and the conversion noise between TACs and FDCs are relatively small, so each one can be ignored, as shown in Fig. 5(b). In addition, the transmitted noise from SCs increases, and the transmitted noise from TACs decreases. Similarly, as g_2 increases, the intrinsic noise of FDCs, the conversion noise between SCs and TACs, and that between TACs and FDCs are so small that each can be ignored, as shown in Fig. 5(d). In addition, the transmitted noise from SCs decreases, while that from TACs increases.

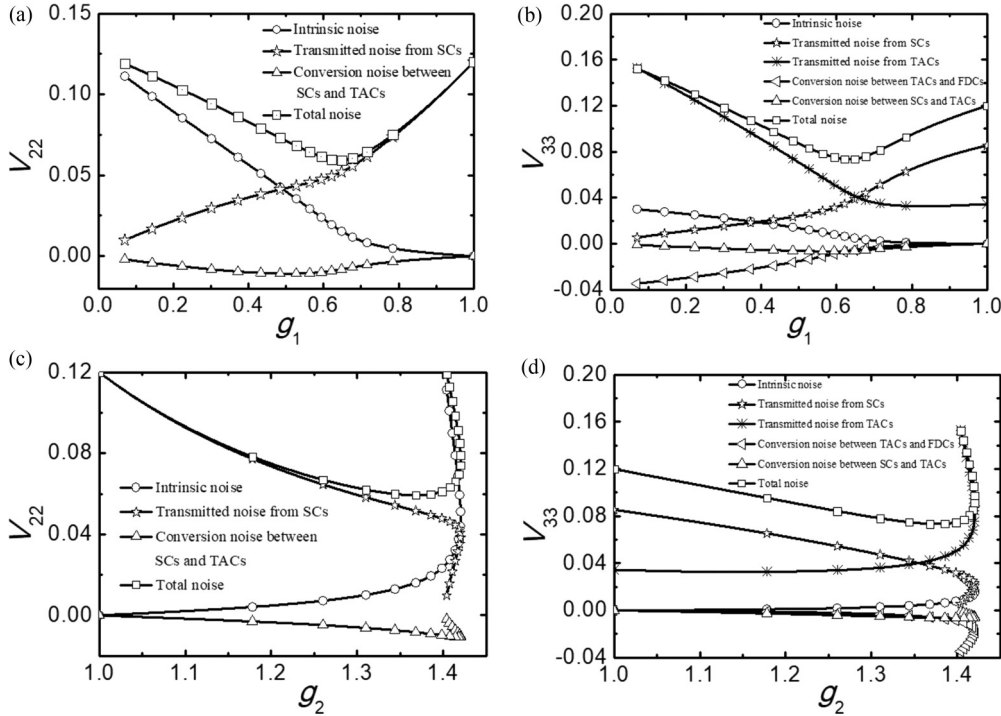


FIG. 5. Effects of gain factors g_k ($k = 1, 2$) on noise propagations in cell states cascade in colonic crypt. Lines are theoretical predictions according to Eqs. (26) and (27). Hollow markers are from simulations using the Gillespie method [39]. The other parameter values are given in the text. All the parameters are measured in hours⁻¹.

Therefore, whether for g_1 or g_2 , the total noise in FDCs mainly depends on transmitted noise from SCs and TACs.

Consequently, the transmitted noise is an important component of the total noise in each downstream cell. If the cell population is not too small, it will only cause the small intrinsic noise. Due to the transmitted noise coming from the upstream cell, the total noise is not necessarily small.

E. Effects of gain factor on noise amplification

The three-dimensional graphs of α , g_k ($k = 1, 2$) and noise amplification rate A_i ($i = 1, 2, 3$) are shown in Figs. 6(a) and 6(c). The corresponding projection of each graph on the g_k - A_i plane is shown in Figs. 6(b) and 6(d). It is found from Fig. 6(b) that the values of A_1 and A_3 are both less than 1, which indicates that the noise from SCs to TACs or to FDCs is attenuated. With the increase of g_1 , the values of A_1 or A_3 increase, which means that the attenuation strength is weakened, and finally the noise of TACs or of FDCs is the same as that in SCs. Meanwhile, the value of A_2 is greater than 1, which suggests that the noise from TACs to FDCs is amplified. With the increase of g_1 , the amplification intensity decreases to the minimum at $g_1 = 0.56$, then increases to the maximum at $g_1 = 0.71$, and finally decreases to 1.

It is found from Fig. 6(d) that the values of A_1 and A_3 are all less than 1, which indicates that the noise is attenuated from SCs to TACs and FDCs. With the increase of g_2 , the value of A_1 or A_3 first decreases linearly, and then decreases rapidly nearly at $g_2 = 1.42$, until to the minimum 0.2, which means that the attenuation intensity first decreases slowly, and then suddenly decreases to a minimum.

Meanwhile, the value of A_2 is greater than 1, which indicates that the noise is amplified from TACs to FDCs. And, the amplification intensity increases to the maximum at $g_2 = 1.28$, then decreased to the minimum at $g_2 = 1.42$, and finally increased until to 1.14.

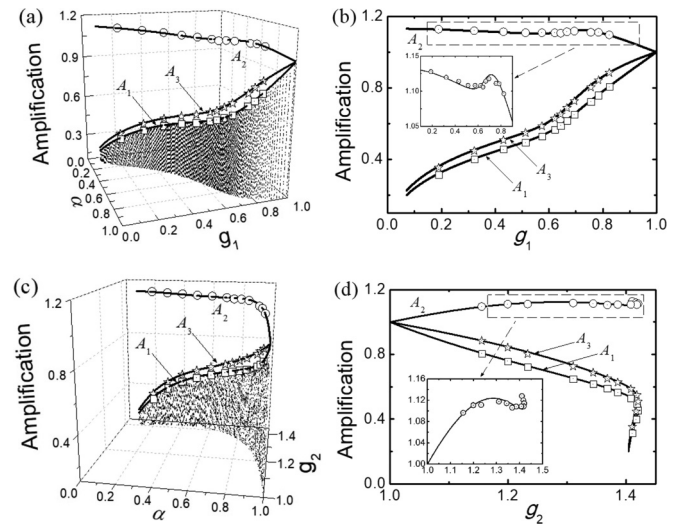


FIG. 6. Effects of gain factors g_k ($k = 1, 2$) on noise amplification rates A_i ($i = 1, 2, 3$). (a), (c) Three-dimensional figure of α , g_k , and A_i ($i = 1, 2, 3$). (b), (d): Corresponding projection figures on the g_k - A_i plane. Lines are theoretical predictions according to Eq. (31). Hollow markers are from simulations using the Gillespie method [39]. The other parameter values are given in the text. All the parameters are measured in hours⁻¹.

Therefore, with the increasing of g_1 or g_2 , the noise is always amplified from TACs to FDCs, and attenuated from SCs to TACs or to FDCs. Reasonable selection of gain factors can effectively adjust the noises of TAC and FDC.

V. CONCLUSIONS AND DISCUSSION

Signal transduction plays an important role in communication between cells. It can affect cell survival, proliferation, differentiation, and death behavior. Like genes and proteins, cells can use biochemical networks to sense and process information [29]. In order to quantitatively describe the relationship between the noise of cells in biochemical networks and the amplification of signals, we choose a unidirectional phenotypic transition cascade in a colonic crypt [34–36] as an example of a stochastic computation system. Taking upstream cells as input signals and downstream cells as output signals, the gain-fluctuation equation is obtained by introducing gain factors. Through the simulation of these theoretical formulas, the characters of noise propagation and amplification are studied.

Different from most works based on the gene level, our work is based on the cellular level in studying the characters of noise propagation and amplification. Different from the gene expression cascade, the input and output signals in our work are affected by biochemical reaction process, rather than a simple numerical change. So, the results are very interesting.

On the one hand, because of the influence of the transmitted noise, the total noise would be large even if the number of cells is large. The influence of the transmitted noise may be the indirect cause of colon cancer. Therefore, no matter whether the number of cells is large or small, the influence of noise on biological system dynamics behavior should be considered. On the other hand, the total noise of the downstream cells always has a minimum value. Therefore, we can intervene in the uncontrollable growth of tumor cells and effectively control the deterioration of colon cancer by selecting a reasonable value of the gain factor. The above conclusions may provide a theoretical basis for clinical control or treatment of colon cancer.

Our work is mainly focused on the unidirectional transition cascade in which upstream cells can transform into downstream cells, but not vice versa. For a bidirectional transition cascade, such as the interconversion between three cell states in breast cancer lines [42] or the transitions between two species in a bacterial community with exploitative competition [43], the interconversion between different cells provides a more complicated random environment. It would be highly interesting to investigate the characters of noise propagation and amplification in our future works.

ACKNOWLEDGMENT

This work was supported by the National Natural Science Foundation of China under Grant No. 11605014 (to Q.-m.P).

-
- [1] G. Li and H. Qian, *Cell Biochem. Biophys.* **39**, 45 (2003).
 - [2] K. L. Dunn, P. S. Espino, B. Drobnic, S. He, and J. R. Davie, *Biochem. Cell Biol.* **83**, 1 (2005).
 - [3] J. D. Thatcher, *Sci. Signal.* **3**, tr1 (2010).
 - [4] O. Pulkkinen and R. Metzler, *Sci. Rep.* **5**, 17820 (2015).
 - [5] S. Reuveni, M. Urbakh, and J. Klafter, *Proc. Natl. Acad. Sci. USA* **111**, 4391 (2014).
 - [6] T. Shibata and K. Fujimoto, *Proc. Natl. Acad. Sci. USA* **102**, 331 (2005).
 - [7] V. Dhananjayulu, V. N. Sagar P, G. Kumar, and G. A. Viswanathan, *PLoS One* **7**, e35958 (2012).
 - [8] C.-C. Wu and B.-S. Chen, in *IEEE International Conference on Fuzzy Systems (FUZZ-IEEE 2011)* (IEEE, 2011).
 - [9] R. Gui, Z. H. Li, L. J. Hu, G. H. Cheng, Q. Liu, J. Xiong, Y. Jia, and M. Yi, *Chin. Phys. B* **27**, 028706 (2018).
 - [10] R. Gui, Q. Liu, Y. Yao, H. Y. Deng, C. Z. Ma, Y. Jia, and M. Yi, *Front. Physiol.* **7**, 600 (2016).
 - [11] A. Hilfinger, T. M. Norman, and J. Paulsson, *Cell Syst.* **2**, 251 (2016).
 - [12] L. S. Tsimring, *Rep. Prog. Phys.* **77**, 026601 (2014).
 - [13] K. H. Kim, H. Qian, and H. M. Sauro, *J. Chem. Phys.* **139**, 144108 (2013).
 - [14] G. Viswanathan, C. Jayaprakash, S. C. Sealfon, and F. Hayot, *Phys. Biol.* **5**, 046002 (2008).
 - [15] T. Shibata and M. Ueda, *Bio. Syst.* **93**, 126 (2008).
 - [16] Y. Miyanaga, S. Matsuoka, T. Yanagida, and M. Ueda, *BioSystems* **88**, 251 (2007).
 - [17] M. Ueda and T. Shibata, *Biophys. J.* **93**, 11 (2007).
 - [18] D. Zhao, S. Liu, and Y. Gao, *Acta. Biochim. Biophys. Sin. (Shanghai)* **50**, 231 (2018).
 - [19] Y. Sako, S. Minoguchi, and T. Yanagida, *Nat. Cell Biol.* **2**, 168 (2000).
 - [20] H. Qian, *Annu. Rev. Biophys.* **41**, 179 (2012).
 - [21] P. J. Choi, L. Cai, K. Frieda, and X. S. Xie, *Science* **322**, 442 (2008).
 - [22] M. Thattai and A. van Oudenaarden, *Biophys. J.* **82**, 2943 (2002).
 - [23] P. B. Detwiler, S. Ramanathan, A. Sengupta, and B. I. Shraiman, *Biophys. J.* **79**, 2801 (2000).
 - [24] O. G. Berg, J. Paulsson, and M. Ehrenberg, *Biophys. J.* **79**, 1228 (2000).
 - [25] J. Paulsson, O. G. Berg, and M. Ehrenberg, *Proc. Natl. Acad. Sci. USA* **97**, 7148 (2000).
 - [26] J. Paulsson and M. Ehrenberg, *Phys. Rev. Lett.* **84**, 5447 (2000).
 - [27] J. Paulsson, *Nature (London)* **427**, 415 (2004).
 - [28] X. Zheng and Y. Tao, *J. Chem. Phys.* **128**, 165104 (2008).
 - [29] G. Hornung and N. Barkai, *PLoS Comp. Biol.* **4**, e8 (2008).
 - [30] H. Zhang, Y. Chen, and Y. Chen, *PLoS One* **7**, e51840 (2012).
 - [31] G. Rieckh and G. Tkačik, *Biophys. J.* **106**, 1194 (2014).
 - [32] D. A. Oyarzún, J. B. Lugagne, and G. B. V. Stan, *ACS Synth. Biol.* **4**, 116 (2014).
 - [33] M. D. Harton and E. Batchelor, *J. Mol. Biol.* **429**, 1143 (2017).
 - [34] M. D. Johnston, C. M. Edwards, W. F. Bodmer, P. K. Maini, and S. J. Chapman, *Proc. Natl. Acad. Sci. USA* **104**, 4008 (2007).

- [35] Q. M. Pei, X. Zhan, L. J. Yang, J. Shen, L. F. Wang, K. Qui, T. Liu, J. B. Kirunda, A. A. M. Yousif, A. B. Li, and Y. Jia, *Phys. Rev. E* **92**, 012721 (2015).
- [36] Q. M. Pei, X. Zhan, L. J. Yang, C. Bao, W. Cao, A. B. Li, A. Rozi, and Y. Jia, *Phys. Rev. E* **89**, 032715 (2014).
- [37] J. Paulsson, *Phys. Life Rev.* **2**, 157 (2005).
- [38] D. T. Gillespie, *J. Phys. Chem.* **81**, 2340 (1977).
- [39] N. G. van Kampen, *Stochastic Processes in Physics and Chemistry, 2nd ed.* (Elsevier, Amsterdam, 1997).
- [40] T. Brett and T. Galla, *Phys. Rev. Lett.* **110**, 250601 (2013).
- [41] P. B. Warren, *Phys. Rev. E* **80**, 030903(R) (2009).
- [42] P. B. Gupta, C. M. Fillmore, G. Jiang, S. D. Shapira, K. Tao, C. Kuperwasser, and E. S. Lander, *Cell* **146**, 633 (2011).
- [43] J. Mao, A. E. Blanschard, and T. Lu, *ACS Synth. Biol.* **4**, 240 (2015).